International Journal of Recent Technology and Engineering (IJRTE)
ISSN: 2277-3878 (Online), Volume-8 Issue-2, July 2019

Corrosion Inhibitor Performance of Phenol Derivative using Density Functional Theory

Muhamad Husaini Abu Bakar, Mohamad-Syafiq Mohd-Kamal, Sazali Yaacob

Abstract: ***Metal-air batteries are demanded in nowadays as a potential replacement of lithium based batteries in storage applications. Because of corrosion occur in metal electrode, this corrosion limited the performance lifetime of the metal-air batteries. The aims of this paper to evaluate the performance inhibition efficiency of phenol derivatives using quantum approach. An inhibitors efficiency of eight phenol derivatives was calculated using Density Functional Theory (DFT) with B3LYP functional and 6-311(d,p) basis set. The parameter of electronic structure was calculated to determine the inhibition efficiency. All of the phenol derivatives led to an increase in inhibition efficiency except 5-Methyl-2-nitrophenol and 4-(Methoxycarbonyl)phenol. DFT show that Phenol, 2,6-dimethoxy-4-2-(2-propenyl) is higher inhibitor efficiency at 94%. As a conclusion, phenol derivatives extracted from the pyrolysis can be used as inhibitor to reducing the corrosion on metal.***

Index Terms: ***Density Functional Theory, HOMO-LUMO, Organic Inhibitor, B3LYP.***

I. INTRODUCTION

The increasing demand for metal-air batteries has attracted researchers to study corrosion inhibitors. The main problem of the metal-air battery is high corrosion in the anode [1, 2]. Several types of inorganic inhibitors have been introduced, such as sodium salts of molybdate, tungstate, and vanadate, to reduce the corrosion rates at the metal [3, 4]. However, inorganic inhibitors have the potential to produce highly toxic products, and therefore, endanger human health [4]. This toxic problem limits the use of inorganic inhibitors for controlled applications. As the application of metal-air batteries is widespread in the present era, including for electric vehicles, such toxicity is inflexible. Thus, studies concerning organic inhibitors are indeed a pressing need.

Organic inhibitors have several advantages over inorganic inhibitors, particularly its low levels of toxins [5–7]. Organic inhibitors can be extracted from various agricultural by-products [8]. Through the pyrolysis process, agricultural waste sources can be separated into useful chemical compounds. Kabir, G. et al., (2017) claimed that organic chemical compounds could be generated from mesocarp oil palm. This discovery opens an excellent opportunity to identify suitable organic inhibitors for use in metal-air batteries.

Although many researchers have revealed that chemical compounds can be produced by the process of pyrolysis, only a handful seems to associate this discovery with inhibitors. This is mostly due to the lack of knowledge in the electronic structure of the compound itself. Therefore, this paper analysed the inhibitor efficiency of chemical compound from the lens of DFT. The DFT methods were required to obtain a better understanding of the theory related to organic compounds. DFT calculation can help in finding the appropriate organic inhibitor with more practical and fast [10–12].

II. COMPUTATIONAL DETAILS

A.Review Stage

Density Functional Theory (DFT) approach are able to optimise molecule structures and calculate the corrosion inhibitor efficiency quantum parameters such as HOMO, LUMO, electron affinity and ionization potential [13–15]. The combination of the Becke three-parameter hybrid (B3) exchange functional with the Lee-Yang-Parr (LYP) correction functional (B3LYP) and 6-311G(d,p) basis-set was utilised for all geometry optimisation, HOMO, LUMO, and electronic properties [16–18]. This technique was successfully applied to describe the phenol structural of corrosion inhibitors and efficiency on aluminium surfaces [18]. Figure 1 illustrates the selected eight phenol derivatives, which are phenol 2-ethyl, phenol 4-methoxy-3, phenol, 4-ethyl-2, 5-methyl-2 nitrophenol, phenol 2,6- dimethoxy, phenol, 2,6-dimethoxy-4-(2-propenyl), and 4-(Methoxycarbonyl) phenol [8].

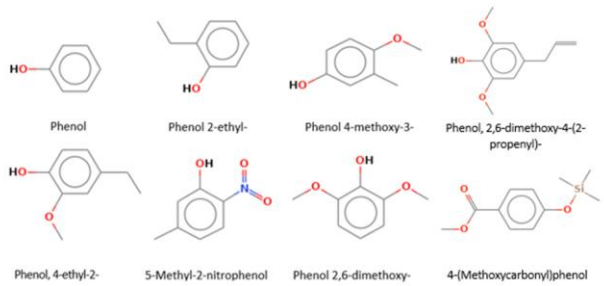

Fig. 1. The structures of phenol derivatives are pyrolysis product.

Revised Manuscript Received on 30 July 2019.

***** Correspondence Author

Muhamad Husaini Abu Bakar*, Head of Research and Innovation, System Engineering and Energy Laboratory (SEELAB), Universiti Kuala Lumpur – Malaysian Spanish Institute, Kulim Hi-Tech Park, Malaysia.

Mohamad-Syafiq Mohd-Kamal, System Engineering and Energy Laboratory (SEELAB), Universiti Kuala Lumpur – Malaysian Spanish Institute, Kulim Hi-Tech Park, Malaysia.

Sazali Yaacob, Electrical and Electronics department, Universiti Kuala Lumpur – Malaysian Spanish Institute, Kulim Hi-Tech Park, Malaysia.

B. Optimization geometry of phenol derivatives

The HOMO and LUMO orbitals are the pair closest to the orbital energy in the molecules of phenol derivatives, which allow them to interact actively. The energy gap depends on energy HOMO and LUMO [19]. When the energy gap is higher, the efficiency of the inhibitor is lowered. Figure 2 shows the optimal geometric structure for phenol derivatives. Molecular orbital for each HOMO and LUMO are different due to movement of electron on molecules [20].

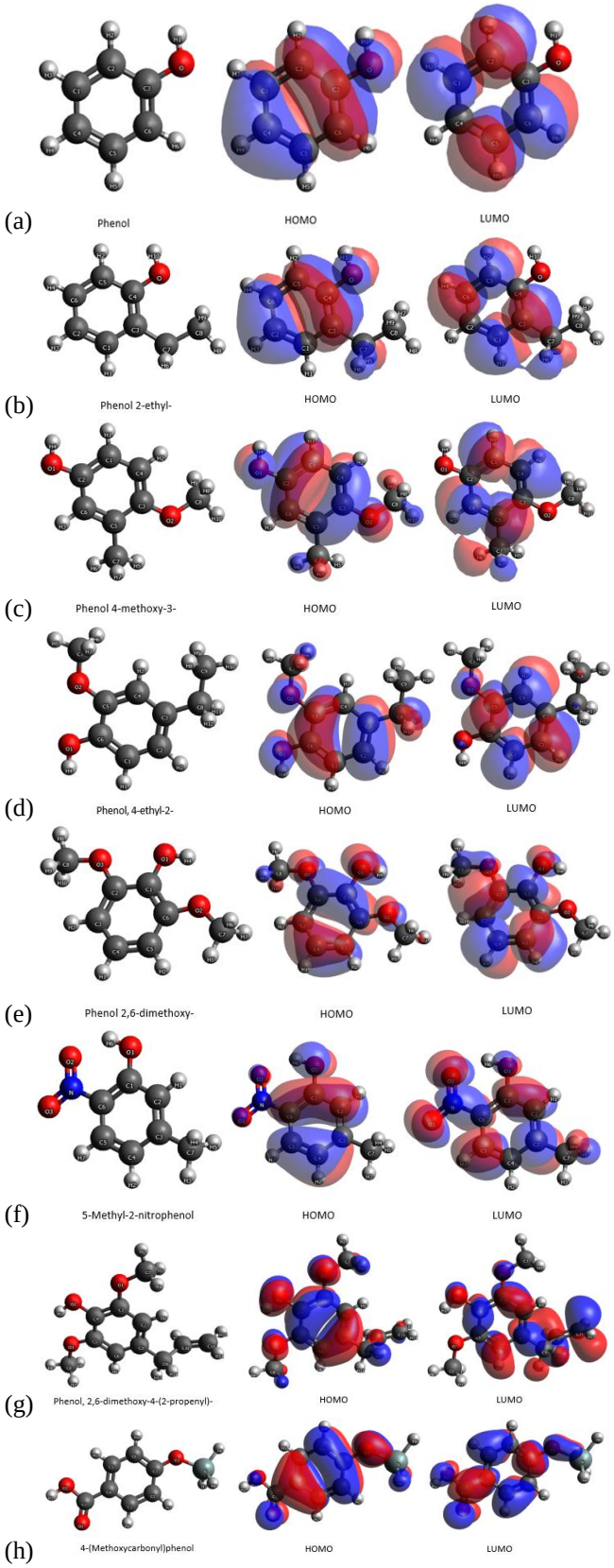

Fig. 2. DFT calculation was performed of optimized geometry structure, HOMO and LUMO molecules structure. a) phenol, b) phenol 2-ethyl, c) phenol 4-methoxy-3-, d) phenol, 4-ethyl-2-, e) phenol 2,6-dimethoxy-, f) 5-methyl-2-nitrophenol, g) Phenol, 2,6-dimethoxy-4-2-(2-propenyl), and 4-(Methoxycarbonyl)phenol.

Figure 2(a) shows the HOMO and LUMO orbital calculations for phenol, where the red color denotes a positive base, while blue for a negative base in the electron orbital. The formation of the size molecule will show how the orbital is produced at HOMO and will affect LUMO in the orbital bond. HOMO-LUMO energy phenol 2-ethyl appeared to be better than phenol molecules because the energy in phenol 2-ethyl donated more electrons. Figure 2(c) presents HOMO-LUMO for the structure of Phenol 4-methoxy-3, which seemed to be increased due to the presence of methoxymethane and ethane in this structure that implies a higher orbit of energy. The structure of Phenol 2,6-dimethoxy is as illustrated in Figure 2(e), where the structure refers to a combination of phenol and 2-methoxymethane. Different HOMO and LUMO for the structure of phenol 2,6-dimethoxy looked small, and it was likely that these molecules gained lower reactions during corrosion.

Electronic method

The computational parameters DFT used to obtain molecules are the energy HOMO and LUMO orbital and the energy gap [18, 22] . The value of electron affinity and ionization potential for phenol derivatives are studied from HOMO and the LUMO energy orbital [22]. Energy HOMO and LUMO can convert orbital energy bonds and relate them to corrosion inhibitors [23].

The value of the gap energy is calculated using, E gap = ELUMO - EHOMO, the energy difference implies the effect reactivity of the chemical species when the value is higher [24]. According to Obayes, H.R. et al. (2014) good inhibition efficiency in molecules when the values of energy gap are low. This energy gap is because the energy of the last occupied orbital will release the electrons for donations to the empty orbital without metal [25].

$$IP = -E_{HOMO} \quad (1)$$

$$EA = -E_{LUMO} \quad (2)$$

The ionization potential (IP) and the electron affinity (EA) are related to the energy of HOMO and LUMO, respectively, within the framework of Koopmans' theorem [28, 29]. This theorem determines the value (IP) and (EA) of the relationship between HOMO and the LUMO energy.

$$\chi = -\mu = \frac{IP+EA}{2} E_{HOMO} \quad (3)$$

$$\eta = \frac{IP-EA}{2} E_{HOMO} \quad (4)$$

$$S = \frac{1}{\eta} E_{HOMO} \quad (5)$$

Theoretically, the parameters of IP and EA have the potential to obtain values of hardness (η), softness (S), absolute electronegativity (χ), the chemical potential (μ) and electrophilicity index (ω) [18, 26].

Table. 1 The values of HOMO, LUMO, gap energy, ionization potential and electron affinity of phenol derivatives was performed by DFT calculation

Molecules	HOMO	LUMO	Gap Energy	Ionization potential (IP)	Electron affinity (EA)
Phenol	-6.219	-0.314	5.889	6.219	0.314
Phenol 2-ethyl-	-6.011	-0.258	5.753	6.011	0.258
Phenol 2,6-dimethoxy-	-5.375	0.336	5.711	5.375	-0.336
Phenol, 4-ethyl-2-	-5.428	0.149	5.577	5.428	-0.149
Phenol, 2,6-dimethoxy-4-2-(2-propenyl)	-5.413	0.024	5.437	5.413	-0.024
4-(Methoxycarbonyl)phenol	-6.758	-1.380	5.378	6.758	1.380
Phenol 4-methoxy-3-	-5.435	-0.133	5.302	5.435	0.133
5-Methyl-2-nitrophenol	-6.852	-2.722	4.130	6.852	2.722

Therefore, the global reactivity χ, μ, η and S can be determined.

$$\omega = \frac{\mu^2}{2\eta} E_{HOMO} \qquad (6)$$

Electrophilicity (ω) that allows the quantitative classification of the global electrophilic properties of a compound on a relative scale [17]. Efil, K. and Obot, I. B. (2017) have shown ω as a measure of the energy reductions due to the maximum flow of electrons between donors and recipients.

III. RESULT AND DISCUSSION

A.HOMO-LUMO, Ionization Potential, and Electron Affinity

The HOMO energy tends to show that the molecules donate electrons to the receiver molecules corresponding to the low orbital energy [22, 27]. Conversely, the orbital energy of undesirable low electron indicates the ability of molecules to receive electrons. The smaller the LUMO energy, the more likely the molecule will take the electrons [30]. The HOMO values show the propensity of the phenol molecules to explain the electrons of the receptor molecules and LUMO to demonstrate the ability of the molecules to receive electrons.

Table 1 presents the results of energy HOMO-LUMO, energy gaps, IP and EA for phenol derivatives. The difference in energy involves the low or high reactions of phenol derivatives. The result of the energy of HOMO and LUMO for phenol is -6.219 eV and -0.314 eV respectively. The phenol 2,6-dimethoxy shows the highest energy for HOMO and LUMO, that is, -5.375 eV and 0.336 eV. As shown in Figure 2(e), the combination of phenol and 2-methoxymethane in this molecule influences the formation of the HOMO-LUMO. It happens because many reactions are involved in orbital for HOMO-LUMO Phenol 2,6-dimethoxy. Table 2 also shows 5-methyl-2-nitrophenol as the lowest energy for HOMO and LUMO where the values are -6.852 eV and -2.722 eV, respectively. This energy is low because the N-double bond in HOMO for 5-methyl-2-nitrophenol does not remove the electrons as shown in Figure 2(f). It is because the size of the atom is low. The value of molecular energy will be low when the number of atoms is low.

Figure 3 illustrates the value of the energy gap for the phenol derivatives. This energy gap is the value of energy between HOMO and LUMO. The reactivity of the molecule depends on the energy gap, when the energy gap is higher, then the reactivity of molecule is lower [31]. Figure 3 show the value of phenol is 5.889eV because the value of energy gap is high. This result indicates that phenol is a low reactivity of other molecules. The smallest energy gap is 5-methyl-2-nitrophenol where the value is 4.13 eV. The difference in the energy values of 5-methyl-2-nitrophenol and other molecules is very high. This 5-methyl-2-nitrophenol has high reactivity. Although 5-methyl-2-nitrophenol has high reactivity, still cannot show a good attraction.

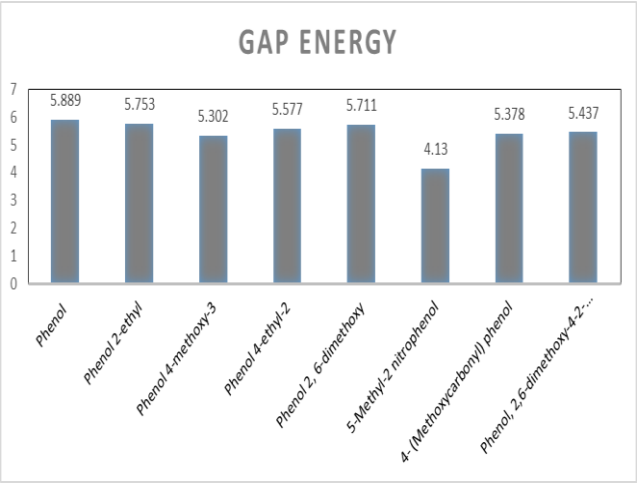

Fig. 3 The gap energy value of phenol derivatives.

Ionization potential (IP) is the energy required to remove electrons from atoms [18, 30]. IP present the molecule stability of molecules. The high value of IP will display the stability of the molecule. Although the molecule is

Table. 2 The value of total energy, dipole moment, absolute electronegativity, hardness, softness, chemical potential, and electrophilicity index of phenol derivatives

Molecules	Parameter						
	Total Energy a.u.	Dipole moment (D)	Absolute electronegativity (χ)	Hardness (η)	Softness (S)	Chemical potential (μ)	Electrophilicity index (ω)
Phenol	-1286.344	0.815	20.326	-18.407	0.340	-20.326	69.916
Phenol,2-ethyl-	-1615.338	2.011	18.788	-17.321	0.348	-18.788	51.708
Phenol,4 methoxy-3	-1932.009	1.589	15.098	-14.116	0.377	-15.098	43.162
Phenol, 4-ethyl-2-	-2094.464	2.002	14.315	-15.136	0.359	-14.315	36.850
Phenol 2,6-dimethoxy	-2244.612	1.036	13.516	-15.346	0.350	-13.516	32.111
5-Methyl-2 nitrophenol	-2306.491	4.896	32.798	-14.132	0.545	-32.798	260.549
2,6, dimethoxy-4-2-(2-propenyl)	-3294.741	9.103	14.596	-18.109	0.416	-27.523	39.115
4-(Methoxycarbonyl)	-2735.624	3.785	27.523	-14.736	0.399	-14.596	140.609

stable, when IP is high, the molecule less is excited. Figure 4 gives the results of IP for phenol derivatives. The value of the phenol IP is 6.219. IP for phenol will be the point of reference for other molecules to know the inhibition efficiency. The IP value of 5-methyl-2-nitrophenol is 6.852, this is higher than those of other molecules, including phenol. It shows that 5-methyl-2-nitrophenol is a very stable molecule. However, the electron of 5-methyl-2-nitrophenol is less excited due to stability is high. The lowest IP value is a 2,6-dimethoxy phenol molecule of 5.375.

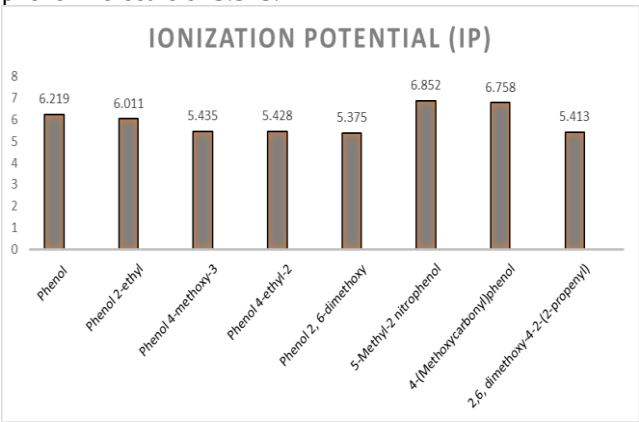

Fig. 4 The ionization potential (IP) values of phenol derivatives.

This phenol 2,6-dimethoxy is the low stability of the other molecules. Even though phenol 2,6-dimethoxy has low stability, but this molecular have high electron excited. The inhibition efficiency will depend on the less stability of the molecule. Therefore, the value of IP will affect the efficacy of this inhibition of phenol derivatives.

B. Electronic structure

The DFT calculation can determine the amount of energy and the dipole moment in the molecule. Table 2 above shows the results of the total energy and the dipole moment for phenol derivatives. The energy for phenol is -1286.34 a.u. The results show that the energy of the phenol derivatives is higher, and the highest energy is 2,6, dimethoxy-4-2-(2-propenyl) which is -3294.74 a.u. Also, Table 2 performs computational hardness (η), softness (S), absolute electronegativity (χ), the chemical potential (μ) and electrophilicity index (ω) for phenol derivatives. This result shows that the highest electrophilicity index was 260.5 of the 5-Methyl-2 nitrophenol molecule and the lowest was 32.1 of Phenol 2,6-dimethoxy.

C. Corrosion Inhibitor Efficiency

Table 3 shows the values of theoretically calculated percentage of inhibition efficiency ($Ie_{theor.}\%$), ionization potential percentage addictive ($I_{add.}\%$) and the inhibition efficiency percentage addictive ($Ie_{add.}\%$) for phenol derivatives. DFT determined the value of IP for phenol derivatives. The IP value were applying to the equation ($I_{add.}\%$). Then, by using equation ($Ie_{add.}\%$) and ($Ie_{theor.}\%$) can determined the value of corrosion inhibitor efficiency.

$$I_{add.}\% = \frac{I_{phenol} - I_{x-phenol}}{I_{phenol}} \; x \; 100\% E_H \qquad (7)$$

Table 3: The values of $I_{add.}\%$, $Ie_{add.}\%$ and $Ie_{theor.}\%$ of phenol derivatives.

Molecules	$I_{add.}\%$	$Ie_{add.}\%$	Inhibition efficiency %	
			Theoretical ($Ie_{theor.}\%$)	Experimental
Phenol	0	0	83.3	83.3*
Phenol 2-ethyl-	2.5	2.1	85.4	-
Phenol 4-methoxy-3-	11.8	9.8	93.1	-
Phenol, 4-ethyl-2-	11.9	9.9	93.3	-
Phenol 2,6-dimethoxy-	12.8	10.7	93.9	-
5-Methyl-2-nitrophenol	-11.2	-9.3	73.9	-
4-(Methoxycarbonyl)phenol	-8.7	-7.2	76.1	-
Phenol, 2,6-dimethoxy-4-2-(2-propenyl)	12.9	10.8	94.0	-

*The value of inhibition efficiency from experiment observed [18].

$$Ie_{add.}\% = I_{add.}\% \; x \; Ie_{phenol}\% \; E_H \quad (8)$$

$$Ie_{theor.}\% = Ie_{add.}\% + Ie_{phenol}\% \; E_H \quad (9)$$

The results show that the inhibitor efficiency of the phenol inhibitor of the phenol derivative in which the efficacy of the experimental value inhibitor for phenol is 83.3%. The value of $I_{add.}\%$ for Phenol 2-ethyl- is 2.5% and the value of $Ie_{add.}\%$ is 2.1%. This molecule Phenol 2-ethyl increases the value of $Ie_{theor.}\%$ that's 85.4%. The value of $Ie_{theor.}\%$ of Phenol 2-ethyl- higher than phenol.

Value $I_{add.}\%$ for Phenol 4-methoxy-3- is 11.8% where the percentage increases very high that Phenol 2-ethyl-. In addition, the value of $Ie_{add.}\%$ increased. This is because the IP value for Phenol 4-methoxy-3 is low. This shows that the value of $I_{add.}\%$ influenced by the IP values because when the IP value is low, the molecular reactivity is high. The value of $Ie_{theor.}\%$ for Phenol 4-methoxy-3- is 93.1%.

The molecule of Phenol, 4-ethyl-2- in Table 3 present the value of $I_{add.}\%$ and $Ie_{add.}\%$ is slightly same with Phenol 4-methoxy-3- where the value is 11.9% and 9.9% respectively. Even though both molecules have the same with the value of IP but the value of energy LUMO for Phenol, 4-ethyl-2- is low stability. This means the most influence to inhibitor efficiency depends on the value of IP. The value of $Ie_{theor.}\%$ for Phenol 4-ethyl-2- is 93.3%.

Also, Table 3 shows the value of $I_{add.}\%$ for Phenol 2,6-dimethoxy- the molecule is 12.8% and the value of $Ie_{add.}\%$ is 10.7%. The result shows Phenol 2,6-dimethoxy- has high value for $Ie_{theor.}\%$ which is 93.9%. The energy HOMO and LUMO orbital shows the energy for Phenol 2,6-dimethoxy- is high. The energy of HOMO and LUMO is effected by inhibitor efficiency for this phenol derivatives.

The difference with the other molecules, molecule for 5-Methyl-2-nitrophenol is to show the value of $I_{add.}\%$ is -11.2% and value of $Ie_{add.}\%$ is -9.3%. This molecule has the lower value than others molecules. This is because the value IP of 5-Methyl-2-nitrophenol is high then the value IP of phenol. When the value IP is high, the molecule is very stable but the reactivity is very low. The value of $Ie_{theor.}\%$ is 73.9% where the percentage of this molecule is decreasing.

Molecule for 4-(Methoxycarbonyl)phenol has the same situation with 5-Methyl-2-nitrophenol. The value of inhibition efficiency for 4-(Methoxycarbonyl)phenol is led to decrease. The value of $I_{add.}\%$ is -8.7% and value of $Ie_{add.}\%$ is -7.2%. The value of $I_{add.}\%$ and $Ie_{add.}\%$ will affect the efficiency of the molecule. The decreasing of efficiency present that this 4-(Methoxycarbonyl)phenol still can be use as inhibitor compound but not high efficiency than the other molecules.

Table 3 shows the value of $I_{add.}\%$ for the Phenol, 2,6-dimethoxy-4-2-(2-propenyl) molecule is 12.9% and value of $Ie_{add.}\%$ is 10.8%. The result shows Phenol, 2,6-dimethoxy-4-2-(2-propenyl) has high value for $Ie_{theor.}\%$ which is 94.0%. The energy EHOMO and ELUMO orbital shows the energy for Phenol, 2,6-dimethoxy-4-2-(2-propenyl) is higher than others molecules. The increasing of this molecule inhibitor efficiency indication that Phenol, 2,6-dimethoxy-4-2-(2-propenyl) can be use as inhibitor compound.

IV. CONCLUSION

Organic inhibitors seem to have the potential to reduce toxic problems and to offer corrosion solutions in the anodes of metal-air batteries. Eight phenol derivatives were selected in this study to analyze the organic inhibitors via DFT calculations. The findings of this research show that phenol 2,6-dimethoxy had the highest efficiency of inhibition. Although phenol 2 Phenol, 2,6-dimethoxy-4-2-(2-propenyl) displayed low stability; the reactivity of this molecule was high.

Besides, the lower value of the chemical potential and the electrophilicity index make this molecule an excellent inhibitor. All the phenol derivatives led to an increase in inhibition efficiency, except 5-methyl-2-nitrophenol. This 5-methyl-2-nitrophenol exhibited the lowest efficiency of the barrier. Therefore, it can be concluded that phenol derivatives can improve inhibition efficiency as an organic inhibitor.

ACKNOWLEDGMENT

The authors would like to acknowledge the financial contributions from the Short Term Research Grant STRG program [grant number str17064]. The authors are also grateful to the support given from the Yayasan Tengku Abdullah Scholarship (YTAS) under Universiti Kuala Lumpur.

REFERENCES

1. M. Mokhtar *et al.*, "Recent developments in materials for aluminum-air batteries: A review," *J. Ind. Eng. Chem.*, vol. 32Mokhtar, pp. 1–20, 2015.
2. Y. Liu, Q. Sun, W. Li, K. R. Adair, J. Li, and X. Sun, "A Comprehensive Review on Recent Progress in Aluminum-air Batteries," *Green Energy Environ.*, vol. 2, no. 3, pp. 246–277, 2017.
3. F. Atmani, D. Lahem, M. Poelman, C. Buess-Herman, and M.-G. Olivier, "Mild steel corrosion in chloride environment: effect of surface preparation and influence of inorganic inhibitors," *Corros. Eng. Sci. Technol.*, vol. 48, no. 1, pp. 9–18, 2013.
4. D. S. Kharitonov, I. I. Kurilo, and I. M. Zharskii, "Effect of Sodium Vanadate on Corrosion of AD31 Aluminum Alloy in Acid Media," *Russ. J. Appl. Chem.*, vol. 90, no. 7, pp. 1089–1097, 2017.
5. M. Goyal, S. Kumar, I. Bahadur, C. Verma, and E. E. Ebenso, "Organic corrosion inhibitors for industrial cleaning of ferrous and non-ferrous metals in acidic solutions: A review," *J. Mol. Liq.*, vol. 256, no. 2017, pp. 565–573, 2018.
6. S. U. Ofoegbu *et al.*, "Corrosion inhibition of copper in aqueous chloride solution by 1H-1,2,3-triazole and 1,2,4-triazole and their combinations: electrochemical, Raman and theoretical studies," *Phys. Chem. Chem. Phys.*, vol. 19, no. 8, pp. 6113–6129, 2017.
7. A. Fateh, M. Aliofkhazraei, and A. R. Rezvanian, "Review of corrosive environments for copper and its corrosion inhibitors," *Arab. J. Chem.*, 2017.
8. G. Kabir, A. T. Mohd Din, and B. H. Hameed, "Pyrolysis of oil palm mesocarp fiber and palm frond in a slow-heating fixed-bed reactor: A comparative study," *Bioresour. Technol.*, vol. 241, pp. 563–572, 2017.
9. I. B. Obot, D. D. Macdonald, and Z. M. Gasem, "Density functional theory (DFT) as a powerful tool for designing new organic corrosion inhibitors: Part 1: An overview," *Corros. Sci.*, vol. 99, pp. 1–30, 2015.
10. D. Kim, H. Guk, S. H. Choi, and D. H. Chung, "Benchmarking of computational approaches for fast screening of lithium ion battery electrolyte solvents," *Chem. Phys. Lett.*, vol. 681, pp. 64–68, 2017.
11. V. L. Deringer and G. Csányi, "Machine learning based interatomic potential for amorphous carbon," *Phys. Rev. B*, vol. 95, no. 9, pp. 1–15, 2017.
12. N. Rasool, S. Iftikhar, A. Amir, and W. Hussain, "Structural and quantum mechanical computations to elucidate the altered binding mechanism of metal and drug with pyrazinamidase from Mycobacterium tuberculosis due to mutagenicity," *J. Mol. Graph. Model.*, vol. 80, pp. 126–131, 2018.
13. E. Üstün, Ş. Koç, S. Demir, and I. Özdemir, "Carbon monoxide-releasing properties and DFT/TDDFT analysis of [Mn(CO)3(bpy)L]PF6type novel manganese complexes," *J. Organomet. Chem.*, vol. 815–816, pp. 16–22, 2016.
14. C. Pach, T. Berger, T. Bonte, and D. Trentesaux, "ORCA-FMS: A dynamic architecture for the optimized and reactive control of flexible manufacturing scheduling," *Comput. Ind.*, vol. 65, no. 4, pp. 706–720, 2014.
15. A. Atilgan, Yurdakul, Y. Erdogdu, and M. T. Güllüoğlu, "DFT simulation, quantum chemical electronic structure, spectroscopic and structure-activity investigations of 4-acetylpyridine," *J. Mol. Struct.*, vol. 1161, pp. 55–65, 2018.
16. S. Seyfi, R. Alizadeh, M. D. Ganji, and V. Amani, "Molecular, electronic structure and spectroscopic properties of 6,6′-dimethyl-2,2′-bipyridine and HgI2 complex: Experimental and DFT investigations," *Vacuum*, vol. 139, pp. 9–22, 2017.
17. K. Efil and I. B. Obot, "Quantum chemical investigation of the relationship between molecular structure and corrosion inhibition efficiency of benzotriazole and its alkyl-derivatives on iron," *Prot. Met. Phys. Chem. Surfaces*, vol. 53, no. 6, pp. 1139–1140, 2017.
18. J. D. Talati and R. M. Modi, "O-Substituted Phenols as Corrosion Inhibitors for Aluminium-Copper Alloy in Sodium Hydroxide," *Br. Corros. J.*, vol. 12, no. 3, pp. 180–184, 1977.
19. E. V Shah, C. M. Patel, and D. R. Roy, "Structure, electronic, optical and thermodynamic behavior on the polymerization of PMMA: A DFT investigation," *Comput. Biol. Chem.*, vol. 72, pp. 192–198, 2018.
20. K. Y.-J. O. Y.-H. Byeon Heo-Jin, "Generation of F0 contour using stochastic mapping and vector quantization control parameters," *ICASSP, IEEE Int. Conf. Acoust. Speech Signal Process. - Proc.*, vol. 2, pp. 939–942, 1997.
21. G. Nageswari, G. George, S. Ramalingam, and M. Govindarajan, "Electronic and Vibrational Spectroscopic (FT-IR and FT-Raman) investigation using ab initio (HF) and DFT (B3LYP and B3PW91) and HOMO/LUMO/MEP analysis on the structure of L-serine methyl ester hydrogen chloride," *J. Mol. Struct.*, 2018.
22. M. Alam and S. Park, "Molecular structure, spectral studies, NBO, HOMO–LUMO profile, MEP and Mulliken analysis of 3$β$,6$β$-dichloro-5$α$-hydroxy-5$α$–cholestane," *J. Mol. Struct.*, vol. 1159, pp. 33–45, 2018.
23. H. R. Obayes, G. H. Alwan, A. H. M. J. Alobaidy, A. A. Al-Amiery, A. A. H. Kadhum, and A. B. Mohamad, "Quantum chemical assessment of benzimidazole derivatives as corrosion inhibitors," *Chem. Cent. J.*, vol. 8, no. 1, pp. 2–9, 2014.
24. J. Rezania, H. Behzadi, A. Shockravi, M. Ehsani, and E. Akbarzadeh, "Synthesis and DFT calculations of some 2-aminothiazoles," *J. Mol. Struct.*, vol. 1157, pp. 300–305, 2018.
25. H. R. Obayes, A. A. Al-Amiery, G. H. Alwan, T. A. Abdullah, A. A. H. Kadhum, and A. B. Mohamad, "Sulphonamides as corrosion inhibitor: Experimental and DFT studies," *J. Mol. Struct.*, vol. 1138, pp. 27–34, 2017.
26. W. Wang, N. Wang, P. Li, Y. Bu, X. Xie, and R. Song, "Theoretical studies on the properties of uracil and its dimer upon thioketo substitution," *Theor. Chem. Acc.*, vol. 121, no. 1–2, pp. 21–31, 2008.
27. N. Wazzan, R. M. El-Shishtawy, and A. Irfan, "DFT and TD–DFT calculations of the electronic structures and photophysical properties of newly designed pyrene-core arylamine derivatives as hole-transporting materials for perovskite solar cells," *Theor. Chem. Acc.*, vol. 137, no. 1, 2018.
28. M. Tajbakhsh, M. Kariminasab, M. D. Ganji, and H. Alinezhad, "Molecular design of novel fullerene-based acceptors for enhancing the open circuit voltage in polymer solar cells," *J. Phys. Chem. Solids*, vol. 111, pp. 410–418, 2017.
29. Ö. Mıhçıokur and T. Özpozan, "Molecular structure, vibrational spectroscopic analysis (IR & Raman), HOMO-LUMO and NBO analysis of anti-cancer drug sunitinib using DFT method," *J. Mol. Struct.*, vol. 1149, pp. 27–41, 2017.
30. P. Demir and F. Akman, "Molecular structure, spectroscopic characterization, HOMO and LUMO analysis of PU and PCL grafted onto PEMA-co-PHEMA with DFT quantum chemical calculations," *J. Mol. Struct.*, vol. 1134, pp. 404–415, 2017.
31. M. Alam, M. J. Alam, S. Azaz, M. Parveen, S. Park, and S. Ahmad, "DFT/TD-DFT calculations, spectroscopic characterizations (FTIR, NMR, UV–vis), molecular docking and enzyme inhibition study of 7-benzoyloxycoumarin," *Comput. Biol. Chem.*, vol. 73, pp. 65–78, 2018.
32. Z. Rostami, A. Hosseinian, and A. Monfared, "DFT results against experimental data for electronic properties of C60and C70fullerene derivatives," *J. Mol. Graph. Model.*, vol. 81, pp. 60–67, 2018.

AUTHORS PROFILE

Muhamad Husaini Abu Bakar, is Director for System engineering and Energy Laboratory and Head of Research and Innovation Section at the Universiti Kuala Lumpur – Malaysian Spanish Institute,Malaysia. Having obtained a Bachelor Degree in Manufacturing Engineering with Management at the Universiti Sains Malaysia (2007), Malaysia, he spent the time from 2007–2012 at the Underwater Robotic Research Group, Universiti Sains Malaysia as a research engineer and awarded Master of Science in advance manufacturing from Universiti Sains Malaysia in 2011. Since 2012 he work as lecturer at Universiti Kuala Lumpur – Malaysian Spanish Institute and obtain his Doctor of Philosophy in Advanced Manufacturing from Universiti Sains Malaysia in 2017. His research interests are related to smart manufacturing, energy, and atomistic modelling. He has published over 50 scientific publications in Deep Learning,computational atomistic and metal-air battery. His research activities were recognized by the innovation award of PECIPTA, IIDEX, ICOMPEX, I-ENVEX and MARA due to his innovative invention in smart material and smart monitoring system.

Mohamad-Syafiq Mohd-Kamal, is Master student of System Engineering and Energy Laboratory at the Universiti Kuala Lumpur – Malaysian Spanish Institute,Malaysia. Background of study in Bachelor Engineering Technology (Hons.) Mechatronics at Universiti Kuala Lumpur – Malaysian Spanish Institute. His research interest are related to Quantum Modelling, Energy (Metal-air Batteries), and corrosion inhibitor. His research activities focusing on corrosion inhibitor at aluminium-air battery.

Sazali Yaacob, is Senior Lecturer of Electrical, Electronics & Automation Section at the Universiti Kuala Lumpur – Malaysian Spanish Institute,Malaysia. Background study of Bachelor (Hons.) Electrical Engineering at the Universiti Malaya. Awarded Master of System Engineering at the University of Surrey and having obtained his Doctor of Philosophy in Control Engineering at Sheffield university. His Research area are Satellite Determination and Control System, Intelligent Process Control System, Data analysis and Processing, Biomedical Imaging and Signal Processing, System Identification of Dynamic System, and Acoustic and Image Applications.